

---

# Relocation of electric field domains and switching scenarios in superlattices

L. L. Bonilla, G. Dell'Acqua, R. Escobedo

Universidad Carlos III de Madrid, Leganés, Spain.  
bonilla@ing.uc3m.es

**Summary.** A numerical study of domain wall relocation during slow voltage switching is presented for doped semiconductor superlattices. Unusual relocation scenarios are found and interpreted according to previous theory.

**Key words:** superlattices, relocation of domains, voltage switching

## 1 Introduction

Semiconductor superlattices are essential ingredients in fast nanoscale oscillators, quantum cascade lasers and infrared detectors. Quantum cascade lasers are used to monitor environmental pollution in gas emissions, to analyze breath in hospitals and in many other industrial applications. A semiconductor superlattice (SL) is formed by growing a large number of periods with each period consisting of two layers, which are semiconductors with different energy gaps but having similar lattice constants, such as GaAs and AlAs. The conduction band edge of an infinitely long ideal SL is modulated so that it looks like a one-dimensional (1D) crystal consisting of a periodic succession of a quantum well (GaAs) and a barrier (AlAs). Vertical charge transport in a SL subject to strong electric fields exhibits many interesting features, and it is realized experimentally by placing a doped SL of finite length in the central part of a diode (forming a  $n^+n^-n^+$  structure) with contacts at its ends. In this paper, we study the relocation of electric field domains which appear in a strongly doped, dc voltage biased SL when the voltage is switched between two different values. Our model consists of a system of spatially discrete drift-diffusion equations (DDE) for the electric field and current, an algebraic constraint representing voltage bias, initial and boundary conditions [Bonilla (2002)]. By numerically solving this model, we find that the current through the SL exhibits very different patterns involving several mechanisms for relocating electric field domains, depending on the way the voltage is switched.

## 2 The Sequential Tunnelling Model

We use the discrete drift-diffusion model described in the review paper [Bonilla (2002)]. It consists of the following Poisson and charge continuity equations:

$$F_i - F_{i-1} = \frac{e}{\varepsilon}(n_i - N_D^w), \quad (1)$$

$$\frac{dn_i}{dt} = J_{i-1 \rightarrow i} - J_{i \rightarrow i+1}, \quad (2)$$

for the average electric field  $-F_i$  and the two-dimensional (2D) electron density  $n_i$  at the  $i$ th SL period (which starts at the right end of the  $(i-1)$ th barrier and finishes at the right end of the  $i$ th barrier), with  $i = 1, \dots, N$ . Here  $N_D^w$ ,  $\varepsilon$ ,  $-e$  and  $eJ_{i \rightarrow i+1}$  are the 2D doping density at the  $i$ th well, the average permittivity, the electron charge and the tunnelling current density across the  $i$ th barrier, respectively. The SL period is  $l = d + w$ , where  $d$  and  $w$  are the barrier and well widths, respectively. Time-differencing Eq. (1) and inserting the result in Eq. (2), we obtain the following form of Ampere's law:

$$\frac{\varepsilon}{e} \frac{dF_i}{dt} + J_{i \rightarrow i+1} = J(t). \quad (3)$$

The space-independent unknown function  $eJ(t)$  is the total current density through the SL. Quantum mechanical calculations show that the *constitutive relation* for the tunnelling current density  $eJ_{i \rightarrow i+1}$  is [Bonilla (2002)]

$$J_{i \rightarrow i+1} = \frac{n_i v(F_i)}{l} - D(F_i) \frac{n_{i+1} - n_i}{l^2}. \quad (4)$$

The nonlinear smooth functions of electric field,  $v(F)$  and  $D(F)$  have dimensions of velocity and diffusivity, respectively, and their explicit expressions can be found in Appendix A of [Bonilla (2002)]. It is important to mention that the drift velocity  $v(F)$  has a first local maximum at  $(F_M, v_M)$ , ( $F_M$  and  $v_M$  are both positive), it is positive for positive  $F$ , and  $v(0) = 0$ . Fig. 1 shows  $v/v_M$  as a function of  $F/F_M$ .  $D(F) > 0$  for non-negative  $F$ .

Substituting (1) and (4) in Eq. (3), we find the DDEs:

$$\frac{dF_i}{dt} + v(F_i) \frac{F_i - F_{i-1}}{l} - D(F_i) \frac{F_{i+1} - 2F_i + F_{i-1}}{l^2} = \frac{e}{\varepsilon} \left[ J - \frac{N_D^w v(F_i)}{l} \right], \quad (5)$$

with  $i = 1, \dots, N$ . Bias and boundary conditions are

$$F_0 = F_{N+1} = \rho_c J, \quad \frac{1}{N} \sum_{i=1}^N F_i = \frac{V(t)}{Nl}, \quad (6)$$

in which  $\rho_c > 0$  and  $V(t) > 0$  are the resistivity of the contacts and the voltage, respectively. To analyze this model, it is convenient to render all equations

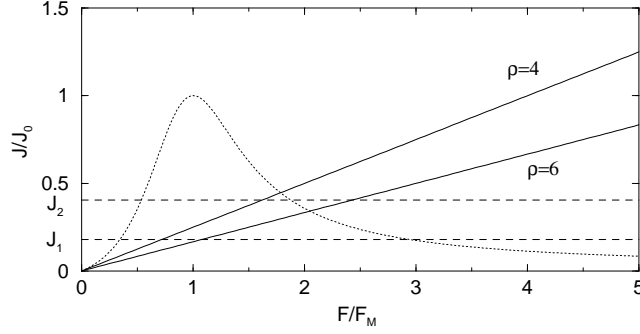


**Fig. 1.** Dimensionless current density (or drift velocity) versus  $F/F_M$  and boundary conditions  $E = \rho J$  for  $\rho = 4$  and  $\rho = 6$ . Stable stationary solutions are found for  $J_1 < J < J_2$  (dashed lines). Current density unit is  $eJ_0 = eN_D^w v_M/l = 2.88 \text{ A cm}^{-2}$ .

dimensionless. We adopt  $F_M$ ,  $N_D^w$ ,  $v_M$ ,  $v_M l$ ,  $eN_D^w v_M/l$  and  $\varepsilon F_M l/(eN_D^w v_M)$  as units of  $F_i$ ,  $n_i$ ,  $v(F)$ ,  $D(F)$ ,  $eJ$  and  $t$ , respectively. Typical SL parameters as in [Amann et al. (2001)] are  $b = 4 \text{ nm}$ ,  $w = 9 \text{ nm}$ ,  $F_M = 6.92 \text{ kV cm}^{-1}$ ,  $N_D^w = 1.5 \times 10^{11} \text{ cm}^{-2}$ ,  $v_M = 156 \text{ cm s}^{-1}$ ,  $v_M l = 2.03 \times 10^{-4} \text{ cm}^2 \text{ s}^{-1}$  and  $eJ_0 = eN_D^w v_M/l = 2.88 \text{ A cm}^{-2}$ . For a circular sample with a diameter of  $120 \mu\text{m}$ , the units of current and time are  $0.326 \text{ mA}$  and  $2.76 \text{ ns}$ , respectively. The nondimensional equations of the model are:

$$\frac{dE_i}{dt} + v(E_i) \frac{E_i - E_{i-1}}{\nu} - D(E_i) \frac{E_{i+1} - 2E_i + E_{i-1}}{\nu} = J - v(E_i), \quad (7)$$

$$\frac{1}{N} \sum_{i=1}^N E_i = \Phi, \quad E_0 = E_{N+1} = \rho J. \quad (8)$$

Here we have used the same symbol for dimensional and dimensionless quantities except for the electric field ( $F$  dimensional,  $E$  dimensionless). The parameters  $\nu = eN_D^w/(\varepsilon F_M)$ ,  $\rho = \rho_c e v_M N_D^w/(l F_M)$ , and  $\Phi = V/(F_M N l)$  are dimensionless doping density, contact resistivity and average electric field (bias), respectively. For the above mentioned 9/4 SL,  $\nu \simeq 3$ . The contact resistivity  $\rho$  will be selected in certain ranges to be specified below and the variation of  $\Phi$  will be explained in the next Section.

### 3 Switching Scenarios

Numerical solution of the Equations (7) - (8) with different initial field profiles shows that (for constant  $\Phi$ ) the stable field profiles  $\{E_i\}$  are time-independent, step-like and increasing with  $i$ : typically they consist of two flat regions called electric field domains separated by an abrupt transition region called a domain wall or charge monopole [Bonilla (2002)]. The current-voltage diagram for these stable solutions is depicted in Fig. 2.

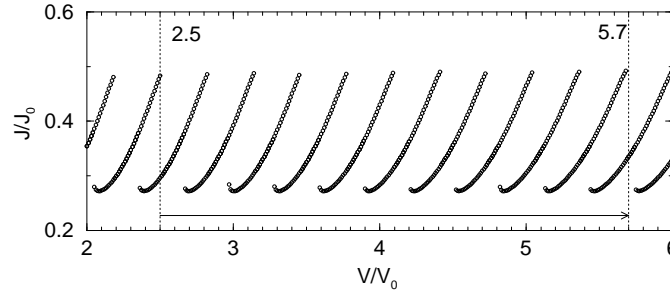


**Fig. 2.** Current–voltage diagram showing stationary branches and applied voltage step. The unit of voltage is 0.36 V.

The electric field profiles of each branch of solutions in Fig. 2 differ in the location of their domain wall: counting branches in the direction of increasing voltage, the profiles of the  $j$ th branch have their domain wall located in the  $(N - j + 1)$ th SL period. Notice that for certain values of the voltage, several branches with different current are possible (multistability). If we switch the voltage from a value  $V_{ini}$  corresponding to one branch to a final value  $V_{fin} = V_{ini} + \Delta V$  corresponding to different branches, the domain wall has to relocate in a different SL period. During switching,  $V(t) = V_{ini} + \dot{V}t$ , with  $\dot{V} = \Delta V/\Delta t$ , and  $\Delta t$  is the ramping time. We now study what happens during switching for different values of  $\Delta t$ .

The case of very small  $\Delta t$  (nanoseconds) and small  $\Delta V$  (spanning two branches) was studied theoretically in [Amann et al. (2001)]. In this paper, we consider much larger values of  $\Delta t$  and  $\Delta V$ , and observe several new phenomena. If  $\Delta t$  is in the range of microseconds and  $\rho$  is appropriate, the current oscillates with time, as shown in Fig. 3 for  $\Delta V$  as depicted in Fig. 2. For a fixed doping density  $\nu$  there are two currents  $J_1$  and  $J_2$  (marked in Fig. 1) such that a domain wall in an infinitely long SL remains stationary if  $J_1 < J < J_2$ , and it moves to the right (resp. left) if  $J < J_1$  (resp.  $J > J_2$ ) [Carpio et al. (2000)].

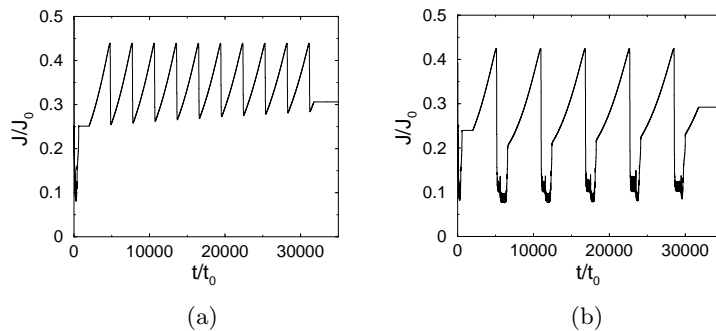


**Fig. 3.** Current density for (a)  $\rho = 4$  and (b)  $\rho = 6$ . The unit of time is 2.76 ns.

Let  $\rho_j$ ,  $j = 1, 2$ , be such that  $v(\rho_j J_j) = J_j$ . During voltage switching, the current changes as in Fig. 3(a) if  $\rho < \rho_1$ , and as in Fig. 3(b) if  $\rho_1 < \rho < \rho_2$ . If  $\rho > \rho_2$ , there are no stationary solutions and the current oscillates periodically in time, as in the Gunn effect [Bonilla (2002)].

Our simulations show that the electric field profile corresponding to Fig. 3(a) consists of slow change of a step-like profile during the finite time intervals in which the current increases followed by a rapid motion of the domain wall, one SL period to the left, when the current is near its local maximum value (which is larger than  $J_2$ ). The domain wall motion is followed by a drop in the current. This situation lasts until the end of switching and the number of maxima of the current is equal to the number of branches skipped during voltage switching. For  $\rho_1 < \rho < \rho_2$ , Fig. 3(b) shows that the number of current maxima during switching is half the (even) number of branches skipped during voltage switching. Near each current maximum (with  $J > J_2$ ), the domain wall traverses one SL period to the left. Immediately afterwards, a pulse of the electric field is created at the injecting left contact and travels to the end of the SL accompanied by the motion of the old domain wall to the right. This is the tripole-dipole scenario discovered in [Amann et al. (2001)] and characterized by a succession of double peaks of the current followed by a succession of single peaks. The novelty is that voltage switching continues after the domain wall has arrived at a stable location and the same process continues until  $t = \Delta t$ . Then the number of current peaks larger than  $J_2$  is half that in Fig. 3(a). If  $\Delta t$  is smaller than a critical value, there is only one large current peak during switching followed by the double peaks - single peak succession typical of only one tripole-dipole scenario.

*Acknowledgement.* We thank B. Birnir, O. Sánchez and J. Soler for fruitful discussions. This work has been supported by the MCyT grant BFM2002-04127-C02, and by the European Union under grant HPRN-CT-2002-00282. R.E. has been supported by a postdoctoral grant awarded by the Autonomous Region of Madrid.

## References

- [Bonilla (2002)] Bonilla, L.L.: Theory of nonlinear charge transport, wave propagation and self-oscillations in semiconductor superlattices. *J. Phys.: Cond. Matter*, **14**, 341 (2002)
- [Amann et al. (2001)] Amann, A., Wacker, A., Bonilla, L.L., Schöll, E.: Dynamic scenarios of multistable switching in semiconductor superlattices. *Phys. Rev. E*, **63**, 066207 (2001)
- [Carpio et al. (2000)] Carpio, A., Bonilla, L.L., Wacker, A., Schöll, E.: Wavefronts may move upstream in semiconductor superlattices. *Phys. Rev. E*, **61**, 4866 (2000)